Ion-Based Quantum Sensor for Optical Cavity Photon Numbers

Moonjoo Lee, Konstantin Friebe, Dario A. Fioretto, Klemens Schüppert, Florian R. Ong, David Plankensteiner, Valentin Torggler, Helmut Ritsch, Rainer Blatt, and Tracy E. Northup

Phys. Rev. Lett. **122**, 153603 — Published 19 April 2019

DOI: 10.1103/PhysRevLett.122.153603

Ion-based quantum sensor for optical cavity photon numbers

Moonjoo Lee,[1] Konstantin Friebe,[1] Dario A. Fioretto,[1] Klemens Schüppert,[1] Florian R. Ong,[1] David Plankensteiner,[2] Valentin Torggler,[2] Helmut Ritsch,[2] Rainer Blatt,[1, 3] and Tracy E. Northup[1, *]

[1]*Institut für Experimentalphysik, Universität Innsbruck, Technikerstraße 25, 6020 Innsbruck, Austria*
[2]*Institut für Theoretische Physik, Universität Innsbruck, Technikerstraße 21, 6020 Innsbruck, Austria*
[3]*Institut für Quantenoptik und Quanteninformation, Österreichische Akademie der Wissenschaften, Technikerstraße 21a, 6020 Innsbruck, Austria*

(Dated: March 26, 2019)

We dispersively couple a single trapped ion to an optical cavity to extract information about the cavity photon-number distribution in a nondestructive way. The photon-number-dependent ac Stark shift experienced by the ion is measured via Ramsey spectroscopy. We use these measurements first to obtain the ion-cavity interaction strength. Next, we reconstruct the cavity photon-number distribution for coherent states and for a state with mixed thermal-coherent statistics, finding overlaps above 99% with the calibrated states.

PACS numbers: 42.50.Pq, 42.50.Ar, 42.50.Lc, 42.50.Nn

Cavity quantum electrodynamics (cavity QED) provides a conceptually simple and powerful platform for probing the quantized interaction between light and matter [1]. Early experiments opened a window into the dynamics of coherent atom–photon interactions, first through observations of collective Rabi oscillations and vacuum Rabi splittings [2–5] and later at the single-atom level [6–11]. More recently, building on measurements of the cavity field via the atomic phase [12, 13], cavity photon statistics have been analyzed in experiments with Rydberg atoms or superconducting qubits in microwave resonators [14–17], culminating in the generation and stabilization of nonclassical cavity field states [18–24]. These experiments operate in a dispersive regime, in which information about the cavity field can be extracted via the qubits with minimal disturbance to the field [1].

Dispersive experiments often operate in a regime in which one photon induces a significant atomic phase shift, the so-called strong pull regime [25]. However, interesting physical phenomena have also been explored with microwave cavities in the weak-pull regime, in which the small phase shift allows partial information about the atomic state to be acquired without collapse onto an eigenstate. Examples include the observation of quantum trajectories [26], the stabilization of Rabi oscillations via quantum feedback [27], and the entanglement of remote qubits [28].

In parallel, it was pointed out that the Jaynes-Cummings Hamiltonian that describes cavity QED also describes the interaction of light and ions in a harmonic trapping potential [29]. This interaction underpins the generation of nonclassical states of motion [30–33] and the implementation of gates between trapped ions [34]. In analogy to the phase shifts experienced by qubits due to the cavity field, ions experience quantized ac Stark shifts due to their coupling to the harmonic trap potential [35]. These shifts have been characterized using techniques similar to those introduced in Ref. [12]. Here, we have transferred the principle of dispersive measurement to an ion qubit coupled to a cavity. In contrast to experiments with flying Rydberg atoms, the ion is strongly confined; in contrast to both Rydberg and superconducting-qubit experiments, our cavity operates in the optical regime.

We employ a single trapped $^{40}\mathrm{Ca}^+$ ion as a quantum sensor [36] to extract information about cavity photons without destroying them. Via Ramsey spectroscopy of the ion, we measure the phase shift and dephasing of the ion's state, both of which result from the interaction of the ion with the cavity field. The mean phase shift is proportional to the mean cavity photon occupation number, due to the ac Stark effect, and the dephasing is due to the cavity photon state not being a pure number state. Reconstructing the cavity photon-number distribution from these measurements allows us to determine the mean and the width of the distribution and thus to distinguish between states with coherent photon statistics and mixed thermal-coherent statistics.

The ion is modelled as a three-level system in which two states, $|S\rangle \equiv |4^2\mathrm{S}_{1/2}, m_J = +1/2\rangle$ and $|D\rangle \equiv |3^2\mathrm{D}_{5/2}, m_J = +1/2\rangle$, comprise a qubit (Fig. 1). The cavity is dispersively coupled to the transition between $|D\rangle$ and the third state, $|P\rangle \equiv |4^2\mathrm{P}_{3/2}, m_J = +1/2\rangle$, with a detuning $\Delta = 2\pi \times 125$ MHz. The quantization axis is defined by a magnetic field of 4.06 G in the plane perpendicular to the cavity axis. The relevant ion-cavity parameters are given by $(g, \kappa, \gamma) = 2\pi\times(0.968, 0.068, 11.5)$ MHz, where g is the ion-cavity coupling strength calculated from the cavity properties and the atomic transition, κ is the cavity field decay rate, and γ is the atomic decay rate of state $|P\rangle$. Here, we assume that the ion is positioned at the waist and in an antinode of a TEM_{00} mode of the cavity [38, 39]. The expected frequency shift of the cavity resonance induced by the dispersively coupled ion is $g^2/\Delta = 2\pi \times 7.50$ kHz, which is much smaller than κ, such that we operate in the weak-

* Corresponding author: tracy.northup@uibk.ac.at

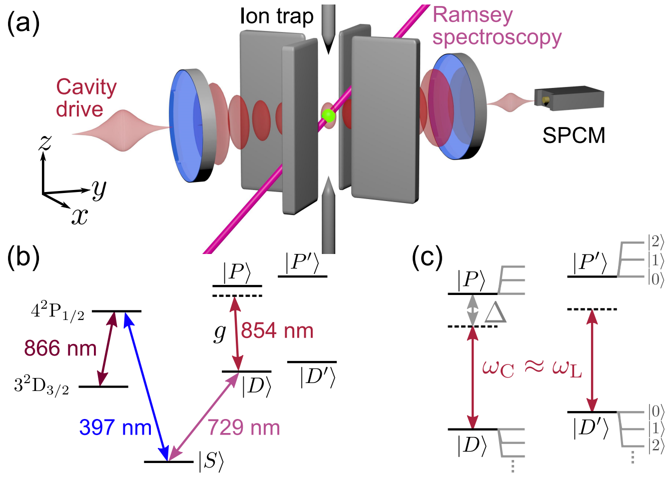

FIG. 1. (a) Experimental set-up. A single ion is coupled to the cavity, which is driven by a weak laser field (cavity drive). The cavity drive laser (along $\hat{y}$) is polarized parallel to the quantization axis, in the direction $\hat{x}+\hat{z}$. The Ramsey spectroscopy laser propagates along $-(\hat{y}+\hat{z})$. Cavity output photons are detected by a single-photon-counting module (SPCM). (b) Energy level diagram of $^{40}Ca^+$ with the relevant levels $|S\rangle$, $|D\rangle$, $|P\rangle$, $|D'\rangle \equiv |3^2D_{5/2}, m_J = +3/2\rangle$ and $|P'\rangle \equiv |4^2P_{3/2}, m_J = +3/2\rangle$ of the ion. The $4^2P_{1/2}$ and $3^2D_{3/2}$ manifolds are used for ion cooling and detection. (c) Levels $|D\rangle$, $|P\rangle$, $|D'\rangle$, and $|P'\rangle$ experience photon-number-dependent ac Stark shifts due to the cavity field, indicated in grey. The frequencies of the bare cavity and the drive laser are ω_C and ω_L, respectively, and Δ is the difference between ω_C and the transition frequency from $|D\rangle$ to $|P\rangle$.

pull regime [25, 26]; see Ref. [37] for further discussion of the choice of Δ. In this regime, the drive laser can be considered to be resonant with the cavity, irrespective of the state of the qubit.

In order to probe the cavity field, the ion is first Doppler-cooled and optically pumped to $|S\rangle$. As the first part of a Ramsey measurement, the qubit is then initialized in a superposition of $|S\rangle$ and $|D\rangle$ by a $\pi/2$-pulse of the Ramsey spectroscopy laser at 729 nm. Next, we drive the cavity with a weak laser field with wavelength $\lambda_L = 854$ nm for $T = 50$ μs. Note that the interaction time T is much larger than the cavity photon lifetime of $\tau_C = 1/(2\kappa) = 1.2$ μs, such that for a mean intracavity photon number of $\langle n\rangle$, $\langle n\rangle T/\tau_C$ photons on average successively interact with the ion. Note also that T is much shorter than the coherence time of 950 μs on the $|S\rangle$–$|D\rangle$ transition [40]. The independently calibrated mean photon number $\langle n\rangle$ of the cavity field is set to a value between 0 and 1.6(3), and the drive laser frequency $\omega_L = 2\pi c/\lambda_L$ is resonant with the cavity frequency $\omega_C + \langle\sigma_D\rangle g^2/\Delta$, where ω_C is the cavity resonance frequency when no ion is coupled to the cavity, and σ_D is the operator for the ion population in $|D\rangle$. Finally, a second $\pi/2$-pulse with variable phase ϕ completes the Ramsey measurement, after which the qubit state is detected using laser fields at 397 nm and 866 nm [40]. The measurement is repeated 250 times for each phase to obtain the ion population in $|D\rangle$.

The mean population in $|D\rangle$ as a function of the phase ϕ is plotted in Fig. 2(a) for three values of $\langle n\rangle$. As $\langle n\rangle$ is increased, two features emerge: the Ramsey fringe is shifted, and its contrast is reduced. The phase shift is directly proportional to $\langle n\rangle$, as shown in Fig. 2(b), with proportionality factor Tg^2/Δ. For $\langle n\rangle = 0.8(2)$ and 1.6(3), the phase of the qubit is shifted by $0.57(3)\pi$ and $1.12(7)\pi$, respectively. A single photon only interacts with the ion during its time in the cavity, which has a mean value τ_C, corresponding to a phase shift of the ion by $\tau_C\, g^2/\Delta = 0.018\pi$. The accumulated effect of all successive photons injected into the cavity accounts for the total phase shift of the qubit.

The measured phase shift as a function of $\langle n\rangle$ can be used to determine the ion-cavity coupling strength. This method is independent of the single-atom cooperativity and thus is valid also for systems in intermediate and even weak coupling regimes. In such regimes, observing the vacuum Rabi splitting is not possible, making it difficult to measure the coupling strength directly. As we have independently determined all ion-cavity parameters and calibrated the photo-detection efficiency, we fit a theoretical model to the data with the coupling strength as the only free parameter. In this way, we extract the experimental value of $g_{exp} = 2\pi \times 0.96(4)$ MHz from the data displayed in Fig. 2(b), in agreement with the theoretical value of $g = 2\pi \times 0.968$ MHz. We performed the same set of measurements on another $^{40}Ca^+$ transition, using the states $|S\rangle$, $|D'\rangle \equiv |3^2D_{5/2}, m_J = +3/2\rangle$, and $|P'\rangle \equiv |4^2P_{3/2}, m_J = +3/2\rangle$ (Fig. 2(c)); the coherence time for the transition $|S\rangle - |D'\rangle$ is 510 μs. For the transition $|D'\rangle - |P'\rangle$, we expect $g' = 2\pi \times 0.790$ MHz and extract $g'_{exp} = 2\pi \times 0.77(4)$ MHz. From the two independent measurements on two transitions, we thus see that this new method determines the atom-cavity coupling strength in agreement with theory.

In Fig. 2(d), the fringe contrast, defined as the peak-to-peak value of the fringe divided by twice the fringe offset, is plotted as a function of $\langle n\rangle$ for the transition $|D\rangle - |P\rangle$ and in Fig. 2(e) for the transition $|D'\rangle - |P'\rangle$. This definition of the contrast takes into account that the midpoint of the fringe is not necessarily 0.5, due to spontaneous emission [37]. For $|D\rangle - |P\rangle$, the contrast decreases from 0.99(2) to 0.46(3) as $\langle n\rangle$ increases from 0 to 1.6. This reduction reflects the fact that the intracavity photon number is inherently probabilistic, and in this case, for a coherent drive, follows a Poissonian distribution. The corresponding photon-number fluctuations in the cavity field lead to fluctuations of the qubit transition frequency through the photon-number-dependent ac Stark shift. Note that the observed reduction of contrast can, equivalently, be interpreted as a consequence of the qubit state being measured by the cavity field [14, 25]: Intracavity photons interact dispersively with the qubit before leaking to the environment. The phase of the output photons thus carries information about the qubit state

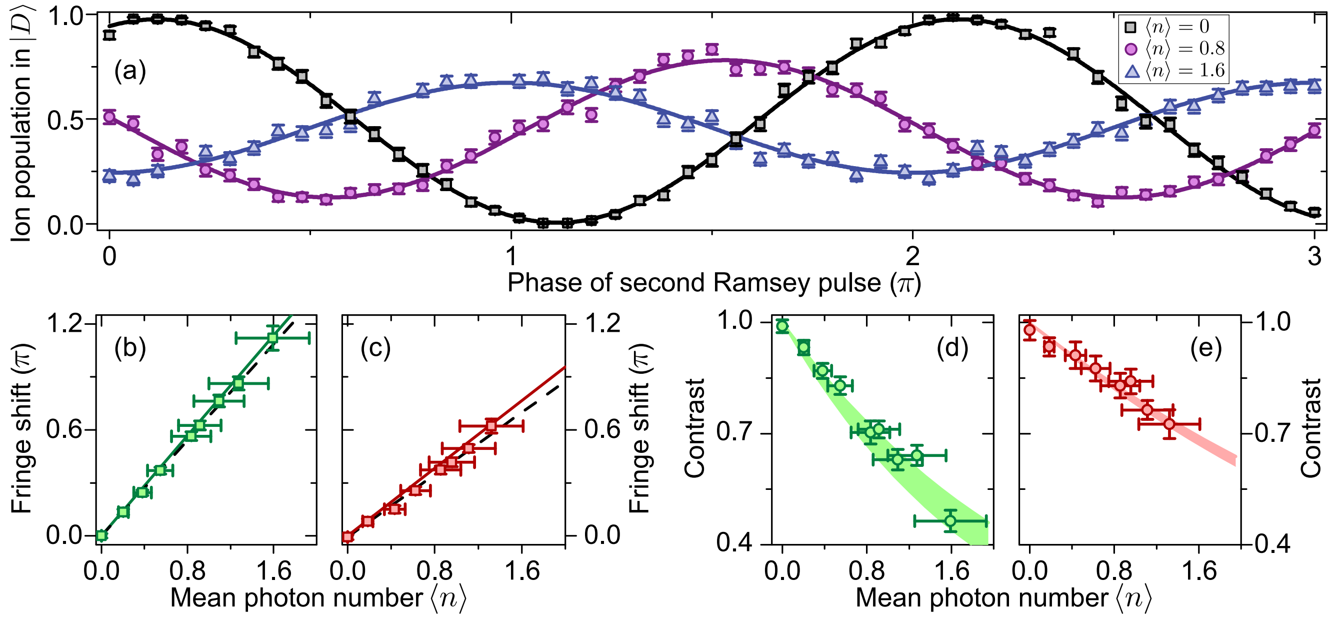

FIG. 2. (a) Ramsey fringes for mean photon numbers $\langle n\rangle = 0$ (black squares), 0.8(2) (purple circles), and 1.6(3) (blue triangles). The solid lines are sinusoidal fits [37] and error bars denote quantum projection noise. (b) The phase shift of the Ramsey fringes as a function of $\langle n\rangle$ for the transition $|D\rangle - |P\rangle$. Squares are experimental data, while the solid line shows the theoretical model using the calculated coupling strength g. The dashed line is a linear fit to the data, from which g_{exp} is extracted (see main text). (c) Ramsey fringe phase shift as a function of $\langle n\rangle$ for the transition $|D'\rangle - |P'\rangle$ with $g' = 0.82\,g$. (d) Contrast of the Ramsey fringes as a function of $\langle n\rangle$ for the transition $|D\rangle - |P\rangle$. The shaded area shows the contrast expected from the theoretical model with g_{exp} as input, including its uncertainty. (e) Contrast vs. $\langle n\rangle$ for the transition $|D'\rangle - |P'\rangle$. For (b)-(e), the plotted uncertainties in $\langle n\rangle$ are statistical and systematic uncertainties from the calibration of the photon number. Systematic uncertainties in $\langle n\rangle$ are 20%. Error bars of fringe shift and contrast are uncertainties of the fits to the Ramsey fringes.

that could be accessed, e.g., with homodyne or heterodyne detection. All such quantum measurements imply some amount of backaction [25], which in our case takes the form of qubit decoherence. Note that in the absence of a cavity, photons would also induce an ac Stark shift of the ion's states, but due to the weakness of the free-space interaction, the effect would be too small to be measured at the single-photon level.

Spontaneous emission contributes to decoherence for both the cavity-drive measurement of Fig. 2 and free-space measurements. We quantify this effect in a reference measurement using an "ion-drive" configuration: The cavity is translated by a few mm along $\hat{x}$ in order to decouple it from the ion. The ion is driven with a laser beam with frequency $\omega_{\mathrm{L}} = \omega_{\mathrm{C}}$. We perform Ramsey measurements with the cavity interaction replaced by the interaction of the ion with this ion-drive laser. The Ramsey fringe contrast is reduced due to off-resonant excitation of the population from $|D\rangle$ to $|P\rangle$, followed by spontaneous emission. Fig. 3 compares the Ramsey fringe contrast as a function of the phase shift for both the ion-drive and cavity-drive measurements. A given phase shift corresponds to the same ac Stark shift at the ion in both measurements. The contrast of the cavity-drive data is smaller than that of the ion-drive data because in the former case, both spontaneous emission and decoherence induced by the cavity photons play a role. We therefore conclude from this reference measurement that decoherence is not just caused by spontaneous emission; rather, a significant contribution to decoherence of the ion qubit stems from interaction with the cavity field via the backaction of the cavity photons on the ion.

Next, we reconstruct the cavity photon number distribution with a maximum likelihood algorithm [37]. This algorithm finds the photon number distribution that is most likely to have interacted with the ion. It is based on a model, in which the coherent cavity drive with mean photon number n_{coh} is described by an amplitude $\eta = \kappa\sqrt{n_{\mathrm{coh}}}$, and additional number fluctuations are described by a thermal bath with mean photon number n_{th} corresponding to an incoherent contribution to the driving [41]. The photon number distribution of the intracavity field is then determined by the two parameters η and n_{th}. The result of the reconstruction is shown in Fig. 4. For the three Ramsey fringes measured on the $|D\rangle - |P\rangle$ transition, displayed in Fig. 2(a), the reconstruction yields a squared statistical overlap (SSO) $\left(\sum_n \sqrt{p_{\mathrm{rec}}(n)p_{\mathrm{cal}}(n)}\right)^2$ between the reconstructed distribution $p_{\mathrm{rec}}(n)$ and the independently calibrated input state distribution $p_{\mathrm{cal}}(n)$ above 99% (Figs. 4(a)-(c)). The reconstructed state shown in Fig. 4(a) cor-

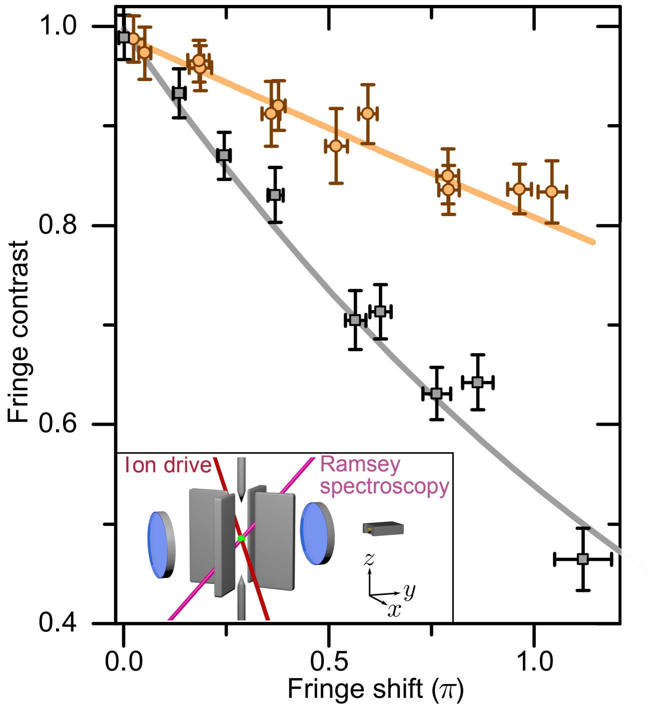

FIG. 3. Ramsey fringe contrast as a function of phase shift for ion-drive (orange circles) and cavity-drive (black squares; same data as in Fig. 2(b) and (d)) measurements on the $|D\rangle$–$|P\rangle$ transition. The lines are theory curves, using g_{exp} for the cavity-drive data. The inset shows the ion-drive beam, which propagates along $\hat{x} - \hat{z}$ and is polarized along $\hat{x} + \hat{z}$, along with the Ramsey spectroscopy beam. The ion is decoupled from the cavity for the ion-drive measurement.

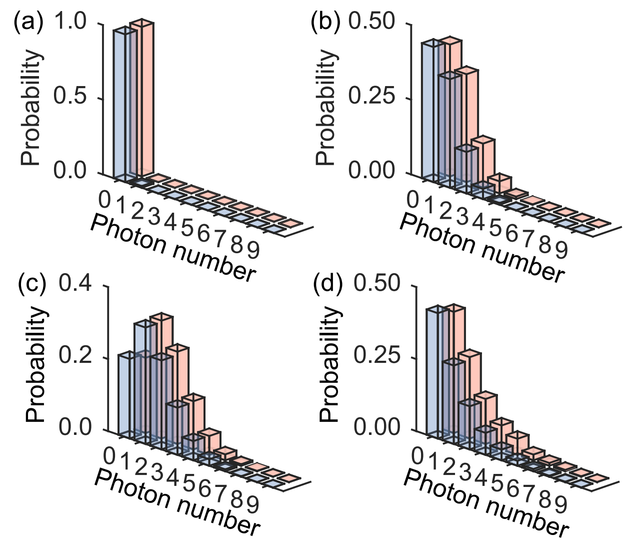

FIG. 4. Photon number distributions reconstructed from the measured Ramsey fringes for intracavity mean photon numbers of (a) 0, (b) 0.8(2), and (c) 1.6(3) (blue bars), and the expected distributions (pink bars). The reconstructed distributions yield mean photon numbers of $0.01^{+0.05}_{-0.02}$, 0.84(8), and $1.49^{+0.05}_{-0.06}$. (d) Reconstructed distribution when the cavity is driven with light of mixed coherent-thermal statistics with mean photon number $\langle n\rangle = 1.05^{+0.07}_{-0.11}$, yielding a reconstructed mean photon number of $\langle n\rangle = 1.12^{+0.14}_{-0.15}$. The squared statistical overlap between the reconstructed distributions and the expected distributions is higher than 0.99 for (a)-(d).

responds to the vacuum state, and the states in Fig. 4(b) and (c) are coherent states, with Mandel Q parameters $Q = \left(\langle n^2\rangle - \langle n\rangle^2\right) / \langle n\rangle - 1$ of $0.00^{+0.02}_{-0.01}$, $-0.03(7)$, and 0.04(5), respectively [42]. The uncertainty of the reconstructed distribution is dominated by quantum projection noise in the Ramsey measurement [37].

This reconstruction method is also applied to a fourth state which is generated by applying amplitude noise to the cavity drive laser via an acousto-optic modulator. The noise has a bandwidth of 10 MHz $\gg 2\kappa$ and can therefore be considered as white noise. The reconstructed state, shown in Fig. 4(d), can be described by mixed coherent and thermal statistics: From the calibration of the added noise [37], a value of $Q = 0.64(6)$ is expected, while the reconstruction yields $Q = 0.70^{+0.07}_{-0.10}$. The result thus shows super-Poissonian intracavity photon statistics caused by the added thermal noise and is clearly distinct from the statistics of a coherent state. Note that our sensing technique is nondestructive because the dispersive interaction with the ion does not annihilate the measured intracavity photons.

An extension of this work would be to reconstruct the full density matrix of arbitrary states of the cavity field. For this purpose, we require a displacement operation of the cavity field, as has been demonstrated in microwave cavities [18]. With the target field to be measured populating the cavity, a second field as a local oscillator would be sent to the cavity. The total field interacting with the ion would be the sum of the known (local oscillator) and unknown (target) fields, and by varying the known field and measuring the state of the ion, one would be able to extract the full target field density matrix.

We have focused here on measuring the ion's state to extract information about the cavity field. However, the scenario can be reversed: quantum nondemolition measurements of the ion's state become possible in our setup via heterodyne measurement of the cavity output field, allowing single quantum trajectories of the ion's electronic state to be monitored and the qubit state to be stabilized, as demonstrated with superconducting qubits [26, 27]. Furthermore, the strong-pull regime ($g^2/\Delta > \kappa$) would be accessible with a higher finesse cavity [25, 26, 37]. In this regime, the qubit spectrum splits into several lines, each corresponding to a different photon-number component [15, 43], providing a route to engineer nonclassical cavity-field states in the optical domain. Other possible extensions include increasing the sensitivity of the measurement by using several ions via their collective coupling to the cavity [44] or via their entanglement [45].

In summary, we have implemented an ion-based analyzer for the statistics of optical photons that does not destroy the photons. Information about the intracavity photon number is imprinted onto the state of an ion qubit via a dispersive interaction. Ramsey spectroscopy and the maximum likelihood method are used to reconstruct the intracavity photon statistics, yielding results in excellent agreement with the expected distributions. Our work represents the first such nondestructive probing of cavity photon distributions in the optical domain, providing tools for the generation of nonclassical optical states.

This work has been financially supported by the Austrian Science Fund (FWF) through Projects F4019, V252, M1964, W1259-N27, and F4013-N23; by the Army Research Laboratory's Center for Distributed Quantum Information via the project SciNet: Scalable Ion-Trap Quantum Network, Cooperative Agreement No. W911NF15-2-0060; and by the European Union's Horizon 2020 research program through the Marie Skłodowska-Curie Actions, Grant No. 656195.

M.L. and K.F. contributed equally to this work.

---

[1] S. Haroche and J. M. Raimond, *Exploring the Quantum: Atoms, Cavities and Photons* (Oxford University Press, New York, 2006).
[2] Y. Kaluzny, P. Goy, M. Gross, J. M. Raimond, and S. Haroche, Phys. Rev. Lett. **51**, 1175 (1983).
[3] M. G. Raizen, R. J. Thompson, R. J. Brecha, H. J. Kimble, and H. J. Carmichael, Phys. Rev. Lett. **63**, 240 (1989).
[4] F. Bernardot, P. Nussenzveig, M. Brune, J. M. Raimond, and S. Haroche, EPL **17**, 33 (1992).
[5] R. J. Brecha, L. Orozco, M. G. Raizen, M. Xiao, and H. J. Kimble, J. Opt. Soc. Am. B **12**, 2329 (1995).
[6] R. J. Thompson, G. Rempe, and H. J. Kimble, Phys. Rev. Lett. **68**, 1132 (1992).
[7] M. Brune, F. Schmidt-Kaler, A. Maali, J. Dreyer, E. Hagley, J. M. Raimond, and S. Haroche, Phys. Rev. Lett. **76**, 1800 (1996).
[8] J. J. Childs, K. An, M. S. Otteson, R. R. Dasari, and M. S. Feld, Phys. Rev. Lett. **77**, 2901 (1996).
[9] C. J. Hood, M. S. Chapman, T. W. Lynn, and H. J. Kimble, Phys. Rev. Lett. **80**, 4157 (1998).
[10] A. Boca, R. Miller, K. M. Birnbaum, A. D. Boozer, J. McKeever, and H. J. Kimble, Phys. Rev. Lett. **93**, 233603 (2004).
[11] P. Maunz, T. Puppe, I. Schuster, N. Syassen, P. W. H. Pinkse, and G. Rempe, Phys. Rev. Lett. **94**, 033002 (2005).
[12] M. Brune, P. Nussenzveig, F. Schmidt-Kaler, F. Bernardot, A. Maali, J. M. Raimond, and S. Haroche, Phys. Rev. Lett. **72**, 3339 (1994).
[13] P. Bertet, A. Auffeves, P. Maioli, S. Osnaghi, T. Meunier, M. Brune, J. M. Raimond, and S. Haroche, Phys. Rev. Lett. **89**, 200402 (2002).
[14] D. I. Schuster, A. Wallraff, A. Blais, L. Frunzio, R.-S. Huang, J. Majer, S. M. Girvin, and R. J. Schoelkopf, Phys. Rev. Lett. **94**, 123602 (2005).
[15] D. I. Schuster, A. A. Houck, J. A. Schreier, A. Wallraff, J. M. Gambetta, A. Blais, L. Frunzio, J. Majer, B. Johnson, M. H. Devoret, S. M. Girvin, and R. J. Schoelkopf, Nature **445**, 515 (2007).
[16] C. Guerlin, J. Bernu, S. Deléglise, C. Sayrin, S. Gleyzes, S. Kuhr, M. Brune, J. M. Raimond, and S. Haroche, Nature **448**, 889 (2007).
[17] B. R. Johnson, M. D. Reed, A. A. Houck, D. I. Schuster, L. S. Bishop, E. Ginossar, J. M. Gambetta, L. DiCarlo, L. Frunzio, S. M. Girvin, and R. J. Schoelkopf, Nature Physics **6**, 663 (2010).
[18] S. Deleglise, I. Dotsenko, C. Sayrin, J. Bernu, M. Brune, J. M. Raimond, and S. Haroche, Nature **455**, 510 (2008).
[19] M. Hofheinz, H. Wang, M. Ansmann, R. C. Bialczak, E. Lucero, M. Neeley, A. D. O'Connell, D. Sank, J. Wenner, J. M. Martinis, and A. N. Cleland, Nature **459**, 546 (2009).
[20] C. Sayrin, I. Dotsenko, X. Zhou, B. Peaudecerf, T. Rybarczyk, S. Gleyzes, P. Rouchon, M. Mirrahimi, H. Amini, M. Brune, J. M. Raimond, and S. Haroche, Nature **477**, 73 (2011).
[21] B. Vlastakis, G. Kirchmair, Z. Leghtas, S. E. Nigg, L. Frunzio, S. M. Girvin, M. Mirrahimi, M. H. Devoret, and R. J. Schoelkopf, Science **342**, 607 (2013).
[22] R. W. Heeres, B. Vlastakis, E. Holland, S. Krastanov, V. V. Albert, L. Frunzio, L. Jiang, and R. J. Schoelkopf, Phys. Rev. Lett. **115**, 137002 (2015).
[23] E. T. Holland, B. Vlastakis, R. W. Heeres, M. J. Reagor, U. Vool, Z. Leghtas, L. Frunzio, G. Kirchmair, M. H. Devoret, M. Mirrahimi, and R. J. Schoelkopf, Phys. Rev. Lett. **115**, 180501 (2015).
[24] C. Wang, Y. Y. Gao, P. Reinhold, R. W. Heeres, N. Ofek, K. Chou, C. Axline, M. Reagor, J. Blumoff, K. M. Sliwa, L. Frunzio, S. M. Girvin, L. Jiang, M. Mirrahimi, M. H. Devoret, and R. J. Schoelkopf, Science **352**, 1087 (2016).
[25] J. Gambetta, A. Blais, D. I. Schuster, A. Wallraff, L. Frunzio, J. Majer, M. H. Devoret, S. M. Girvin, and R. J. Schoelkopf, Phys. Rev. A **74**, 042318 (2006).
[26] K. W. Murch, S. J. Weber, C. Macklin, and I. Siddiqi, Nature **502**, 211 (2013).
[27] R. Vijay, C. Macklin, D. H. Slichter, S. J. Weber, K. W. Murch, R. Naik, A. N. Korotkov, and I. Siddiqi, Nature **490**, 77 (2012).
[28] N. Roch, M. E. Schwartz, F. Motzoi, C. Macklin, R. Vijay, A. W. Eddins, A. N. Korotkov, K. B. Whaley, M. Sarovar, and I. Siddiqi, Phys. Rev. Lett. **112**, 170501 (2014).
[29] C. A. Blockley, D. F. Walls, and H. Risken, EPL **17**, 509 (1992).
[30] J. I. Cirac, R. Blatt, A. S. Parkins, and P. Zoller, Phys. Rev. Lett. **70**, 762 (1993).
[31] D. M. Meekhof, C. Monroe, B. E. King, W. M. Itano, and D. J. Wineland, Phys. Rev. Lett. **76**, 1796 (1996).
[32] C. Monroe, D. M. Meekhof, B. E. King, and D. J. Wineland, Science **272**, 1131 (1996).
[33] D. Kienzler, H.-Y. Lo, B. Keitch, L. de Clercq, F. Leupold, F. Lindenfelser, M. Marinelli, V. Negnevitsky, and J. P. Home, Science **347**, 53 (2015).

[34] H. Häffner, C. Roos, and R. Blatt, Phys. Rep. **469**, 155 (2008).

[35] F. Schmidt-Kaler, H. Häffner, S. Gulde, M. Riebe, G. Lancaster, J. Eschner, C. Becher, and R. Blatt, EPL **65**, 587 (2004).

[36] C. L. Degen, F. Reinhard, and P. Cappellaro, Rev. Mod. Phys. **89**, 035002 (2017).

[37] See Supplemental Material at [URL will be inserted by publisher] for details on how the system is modelled; the reconstruction algorithm; the photon number calibration, including thermal drive; an estimation of the phase resolution; an estimation of spontaneous emission; and a parameter estimation in the strong-pull regime. Supplemental Material includes Refs. [35], [41], and [46-55].

[38] C. Russo, H. G. Barros, A. Stute, F. Dubin, E. S. Phillips, T. Monz, T. E. Northup, C. Becher, T. Salzburger, H. Ritsch, P. O. Schmidt, and R. Blatt, Appl. Phys. B **95**, 205 (2009).

[39] A. Stute, B. Casabone, B. Brandstätter, D. Habicher, P. O. Schmidt, T. E. Northup, and R. Blatt, Appl. Phys. B **107**, 1145 (2012).

[40] P. Schindler, D. Nigg, T. Monz, J. T. Barreiro, E. Martinez, S. X. Wang, S. Quint, M. F. Brandl, V. Nebendahl, C. F. Roos, M. Chwalla, M. Hennrich, and R. Blatt, New J. Phys. **15**, 123012 (2013).

[41] C. Gardiner and P. Zoller, *Quantum Noise: A Handbook of Markovian and Non-Markovian Quantum Stochastic Methods with Applications to Quantum Optics*, Springer Series in Synergetics (Springer-Verlag Berlin Heidelberg, Berlin, 2004).

[42] R. J. Glauber, *Optical Coherence and Photon Statistics* (Wiley-VCH Verlag GmbH & Co. KGaA, 2007).

[43] I. B. Mekhov, C. Maschler, and H. Ritsch, Nat. Phys. **3**, 319 (2007).

[44] S. Begley, M. Vogt, G. K. Gulati, H. Takahashi, and M. Keller, Phys. Rev. Lett. **116**, 223001 (2016).

[45] D. Leibfried, E. Knill, S. Seidelin, J. Britton, R. B. Blakestad, J. Chiaverini, D. B. Hume, W. M. Itano, J. D. Jost, C. Langer, R. Ozeri, R. Reichle, and D. J. Wineland, Nature **438**, 639 (2005).

[46] J. R. Johansson, P. D. Nation, and F. Nori, Comp. Phys. Comm. **183**, 1760 (2012).

[47] J. R. Johansson, P. D. Nation, and F. Nori, Comp. Phys. Comm. **184**, 1234 (2013).

[48] C. W. Gardiner and A. S. Parkins, Phys. Rev. A **50**, 1792 (1994).

[49] H. J. Carmichael, *Statistical Methods in Quantum Optics 1: Master Equations and Fokker-Planck Equations* (Springer-Verlag Berlin Heidelberg, 1999).

[50] A. I. Lvovsky and M. G. Raymer, Rev. Mod. Phys. **81**, 299 (2009).

[51] A. Stute, *A Light-Matter Quantum Interface: Ion-Photon Entanglement and State Mapping*, Ph.D. thesis, Leopold-Franzens-Universität Innsbruck (2012).

[52] W. M. Itano, J. C. Bergquist, J. J. Bollinger, J. M. Gilligan, D. J. Heinzen, F. L. Moore, M. G. Raizen, and D. J. Wineland, Phys. Rev. A **47**, 3554 (1993).

[53] G. Rempe, R. J. Thompson, H. J. Kimble, and R. Lalezari, Opt. Lett. **17**, 363 (1992).

[54] A. H. Myerson, D. J. Szwer, S. C. Webster, D. T. C. Allcock, M. J. Curtis, G. Imreh, J. A. Sherman, D. N. Stacey, A. M. Steane, and D. M. Lucas, Phys. Rev. Lett. **100**, 200502 (2008).

[55] R. Noek, G. Vrijsen, D. Gaultney, E. Mount, T. Kim, P. Maunz, and J. Kim, Opt. Lett. **38**, 4735 (2013).